

Oxidation-Induced Surface Plasmon Band Fragmentation in Silver Clusters

Romain Schira, Franck Rabilloud

▶ **To cite this version:**

Romain Schira, Franck Rabilloud. Oxidation-Induced Surface Plasmon Band Fragmentation in Silver Clusters. Journal of Physical Chemistry C, 2020, 124 (1), pp.968-975. 10.1021/acs.jpcc.9b10898 . hal-02455966

HAL Id: hal-02455966
https://hal.science/hal-02455966

Submitted on 30 Nov 2020

HAL is a multi-disciplinary open access archive for the deposit and dissemination of scientific research documents, whether they are published or not. The documents may come from teaching and research institutions in France or abroad, or from public or private research centers.

L'archive ouverte pluridisciplinaire **HAL**, est destinée au dépôt et à la diffusion de documents scientifiques de niveau recherche, publiés ou non, émanant des établissements d'enseignement et de recherche français ou étrangers, des laboratoires publics ou privés.

Oxidation-Induced Surface Plasmon Band Fragmentation in Silver Clusters

Romain Schira and Franck Rabilloud*

Université de Lyon, F-69003, Lyon, France; Université Lyon 1, Villeurbanne; UMR5306, Institut Lumière Matière

E-mail: franck.rabilloud@univ-lyon1.fr

Abstract

The optical absorption of silver clusters is characterized by a strong plasmon band. However, most of the experimental photoabsorption measurements are performed on clusters interacting with a surrounding media, which can induce oxidation processes and possibly modify the optical properties. Here, we investigate the effects of oxygen adsorption onto the electronic structure and the optical properties of silver Ag_n ($n = 8, 20, 38$) clusters by using a well-established methodology based on the Time-Dependent Density Functional Theory (TDDFT). The presence of oxygen atoms on the silver cluster is found to induce a fragmentation of the plasmon resonance that can lead to its disappearance and the onset of many excitations having a low plasmonic character. The broadening of the plasmon band is shown to depend on the number of oxygen atoms but also on their positions with respect to the cluster. The interaction of Ag_8 clusters with molecular O_2 is also examined. Our study can be used to analyze experimental measurements related to oxygen chemisorption or physisorption on metal clusters, and can also be considered as a first-step to model optical properties of noble metal nanoclusters embedded in oxide matrices.

Introduction

Metallic nanoclusters has been a matter of considerable study for several decades notably because of their unique electronic and optical properties.[1,2] In particular, the Localized Surface-Plasmon Resonance (LSPR) phenomenon, characterized by a very intense absorption band, can be observed on those systems. The LSPR, described as a collective excitation of conduction electrons due to an incident electric field, makes metallic clusters suitable or promising for a wide range of applications, such as photothermal therapy,[3,4] biological sensing,[5] photocatalysis,[6] Surface-Enhanced Raman Spectroscopy (SERS),[7,8] photovoltaics,[9,10] etc.

The LSPR frequency depends on the size, shape, composition[11,12] and environment[13,14]

of the clusters. Even if the LSPR can be investigated on clusters in gas phase[15] most of the experimental photoabsorption measurements are performed on clusters interacting with a surrounding media, i.e., deposited on a surface,[16,17] suspended in a solution,[18] or embedded in solid matrix.[14,19] Trapping allows to obtain a high density and to control the stability of clusters, which facilitates experimental measurements. However, the interactions between the surrounding media and the clusters are complex and generally poorly understood, which makes the analysis of experimental results difficult.[14] Several spectroscopic data obtained on nanometric silver clusters embedded in glass,[20] alumina[21,22] and silica[14,16,23] matrices are referenced in the literature. Globally, oxide matrices cause a red-shift of the LSPR frequency and a broadening of the bandwidth compared to results obtained in gas phase.[13,16] Both the red-shift and the broadening depend on the matrix composition and porosity, and can be described with empirical, semi-classical methods for clusters containing at least a thousand of atoms.[24] Oxide matrices may also induce the formation of Ag-O bonds, a deformation of the cluster, oxidation, and a valence electron confinement. A precise description of those effects, taking into account the details of the atomic structure, is required to trace back the intrinsic properties of the metal cluster. A first-step to correctly model the effects of oxide matrices on a silver cluster is to study the interactions of the cluster with oxygen.

Experimentally, the interaction of oxygen with silver clusters in the gas phase has motived many studies.[25,26] At 77 K molecular oxygen was found to stick chemisorbed to small Ag_n clusters ($n < 70$) with a transfer of one electron, while above 105 K the chemisorption transforms into oxidation, invoking the dissociation of the oxygen molecule.[25] Various theoretical studies using the Density Functional Theory (DFT) focused on the geometrical structure of small oxidized silver. The lowest isomers of charged and neutral Ag_nO_m, with n = 1-6, and m = 1-2 have been determined with a Local Spin Density Approximation (LSDA) exchange-correlation functional.[27] Geometrical structures of clusters containing less than 9 silver atoms in interaction with molecular and dissociated O_2 have been investigated using a Generalized Gradient Approximation (GGA) functional.[28] It appears from those works that

the oxygen atoms can induce important structural deformations in small clusters, and in most cases a dissociative O_2 adsorption is preferred. A more general study of the geometrical structure of neutral and anionic silver clusters containing up to 25 atoms and interacting with molecular oxygen have been realized with GGA and hybrid density-functionals.[29] This study reveals the fact that the binding energy of oxygen atoms and molecular oxygen, as well as ionization potentials and electron affinities follow an odd/even oscillation as a function of cluster size. Absorption spectra of Ag_3O and Ag_4O, and the one of different isomers of Ag_4O, $Ag_{10}O_4$ and $Ag_{10}O_5$, have been computed using the equation-of-motion coupled-cluster (EOM-CC)[30] and Random Phase Approximation (RPA)[31] methods. The authors conclude that the *p*-electrons of oxygen atom activate the *d*-electrons of silver, leading to important changes in the optical response.

None of the previous theoretical works has focused on the effects induced by oxidation on the plasmon resonance in silver clusters. It is well known that the plasmon-like band in silver is clearly visible down to small-size bare clusters of about 18-20 atoms.[19]

To investigate the role of oxidation on the optical response of silver clusters, and especially on the LSPR phenomenon, we examined here the absorption spectra of pure and oxidized Ag_8, Ag_{20} and Ag_{38} in the framework of the Time-Dependent DFT (TDDFT).[32] This method gives precise results on silver clusters provided that an appropriate exchange-correlation functional is used.[19,33–35] For silver clusters, the description of excited states in TDDFT within the adiabatic approximation requires a correction of the self-interaction error (SIE) and a correct asymptotic behaviour. The best results[36] have been obtained with range separated hybrid functionals (RSHs). Those functionals significantly reduce the SIE problems and improve the asymptotic behaviour at long range thanks to the inclusion of Hartree-Fock exchange.[37,38] The present paper is organized as follows: in section 2, we present our approach to generate the geometrical structure of Ag_mO_n (m = 8, 20, 38, and n = 1, 2, 3) and to compute their optical properties. In section 3, we discuss the electronic structure and absorption spectra and we analyze the excited states of pure and oxidized

clusters. This section will finish with a discussion of the effects induced by the dioxygen O_2 onto the optical response of Ag_8.

Computational Method

DFT and TDDFT calculations presented in this paper have been performed with the RSH exchange-correlation functional ωB97x,[39] which includes an increasing part of exact Hartree-Fock exchange at long range (from 16% at short range to 100% at long range). Silver atoms were described with a relativistic effective core potential (RECP), so that only 19 valence electrons per silver atom were treated explicitly ($4s^2$,$4p^6$,$4d^{10}$,$5s^1$), together with the corresponding Gaussian basis set LanL2DZ.[40] The use of this functional and basis set leads to a precise description of the absorption spectra of pure silver clusters and a suitable description on the plasmon phenomenon.[19,36,41] The oxygen atoms have been modelled with the 6-31G* basis set.[42] For molecular oxygen, the use of this basis set leads to a binding energy and bond length of respectively 5.43 eV and 1.20 Å, in good agreement with the experimental ones, referenced as 5.23 eV and 1.21 Å.[28]

The geometrical structures of Ag_8 and Ag_{38} were taken from a study by Chen et al[43] dedicated to the prediction of structures of silver clusters using a genetic algorithm with an embedded atom method potential. Let us note that for Ag_8 we have been considering the two lowest isomers found by Chen et al, respectively of symmetry T_d and D_{2d}, as both of them likely coexist in experimental samples.[41] For the geometrical structure of Ag_{20}, we considered the ground state structure of C_s symmetry optimized at DFT level,[44] this isomer gives an absorption spectra very close to the experimental one.[19] All the geometrical structures were relaxed with ωB97x.

To determine the lowest-energy isomer of the oxidized clusters Ag_mO_n ($m = 8$, 20, 38, and

n = 1, 2, 3), we randomly placed oxygen atoms around the pure silver clusters. For Ag_8O_n, 80 structures have been generated for each value of n ; for half of them, the starting point was Ag_8 in the T_d symmetry, and for the second half it was Ag_8 in the D_{2d} symmetry. For $Ag_{20}O_n$ and $Ag_{38}O_n$, up to 80 structures have been generated for each value of n. Then, we relaxed all the structures with ωB97x and we selected only the lowest-energy isomer for each Ag_mO_n systems for the present study. These are all singlet. Let us note that optimizations of Ag_8O_n that start from Ag_8 with a T_d or D_{2d} symmetry lead to the same lowest-energy isomer.

All DFT and TDDFT calculations were performed using the program Gaussian09.[45] Pre- and post-processing operations were performed by using the graphical interface Gabedit.[46]

Results and discussion

The optimized structures of Ag_8, Ag_{20}, Ag_{38} and Ag_mO_n (m = 8, 20, 38, and n = 1, 2, 3) are presented in Figure 1. Oxygen atoms preferentially stay on the surface. They are adsorbed in 3 or 4-fold position, except for Ag_8O_3 where an oxygen atom is situated between the cluster and a silver atom. The isomer obtained for Ag_8O_2 is already referenced in the literature as being the most steady one.[28] Deformation induced by the presence of O atoms are significant if the number of oxygen atoms is important or if the number of silver atoms is small. The adsorption of a single oxygen atom on Ag_{20} leads to a small elongation of the interatomic distances for Ag atoms bound to the oxygen. The presence of two or three oxygen atoms induces a stronger reorganization in surface while two Ag atoms stay in the core. The adsorption of one or two oxygen atoms on Ag_{38} only induces minor changes in the frame of silver clusters, but a stronger deformation is observed at the surface when three O atoms are adsorbed.

The minimal distance between oxygen and silver atoms, as well as the averaged charge

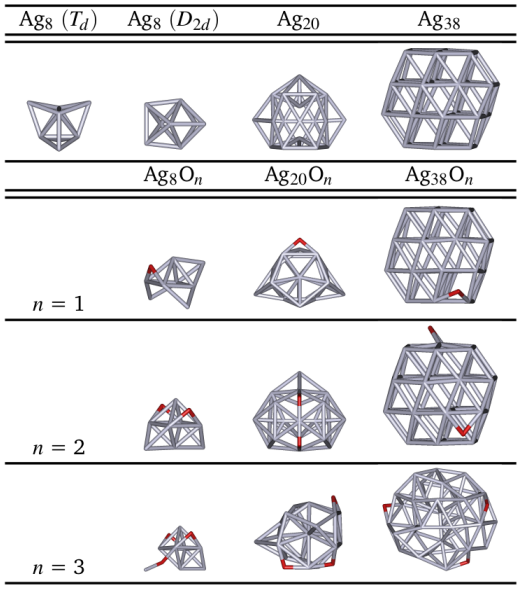


Figure 1: Geometrical structures of pure (Ag_8 with T_d and with D_{2d} symmetry, Ag_{20}, and Ag_{38}) and oxidized (Ag_mO_n, m = 8, 20, 38, and n = 1, 2, 3) silver clusters. The oxygen atoms are represented in red.

and the binding energy of oxygen atoms are referenced in the Table 1. The minimal distance between oxygen and silver atoms varies between 2.09 and 2.24 Å, which is close to the value obtained with LSDA calculation on small oxidized silver clusters.[27] The charges indicate that all oxygen atoms attract at least one electron. Let us note that the present binding energy obtained for Ag_8O_2 is in qualitative agreement with the referenced one.[28]

The absorption spectra of the pure and oxidized silver clusters are presented in Figure 2. The oxygen atoms have an important effect on the optical response of clusters. Absorption of pure silver clusters are dominated by a few intense transitions close to 4.0 eV. When oxygen atoms are present, the few intense transitions are replaced by many transitions having a low oscillator strength and spread over a wide range of energy. A single oxygen atom is enough to produce a significant change in the optical response of Ag_8. The absorption of Ag_8 with symmetry T_d is mainly due to three degenerated transitions situated at 4.04 eV, while the spectrum of the D_{2d}-symmetry structure is dominated by transitions located at 3.74 and 4.00 eV. By contrast, the spectrum of Ag_8O contains many transitions and none

Table 1: Minimal distance between Ag and O atoms (D_{min}, in Å), averaged charge over O atoms (q(O), in $|e|$), and averaged binding energy of O atoms (E_b, en eV) in oxidized silver clusters Ag_mO_n (m = 8, 20, 38, and n = 1, 2, 3). The atomic charge is estimated through the natural population analysis (NPA).[47]

Ag_mO_n		$m = 8$	$m = 20$	$m = 38$
$n = 1$	D_{min}	2.14	2.16	2.24
	q(O)	-1.12	-1.13	-1.22
	E_b	3.07	3.36	4.11
$n = 2$	D_{min}	2.14	2.14	2.18
	q(O)	-1.06	-1.14	-1.17
	E_b	3.37	3.48	3.68
$n = 3$	D_{min}	2.05	2.09	2.12
	q(O)	-1.09	-1.13	-1.18
	E_b	3.26	3.35	3.98

of them can easily be associated to the main one of the pure Ag_8 clusters. The changes in the global appearance induced by a single oxygen atom on the spectra of Ag_{20} and Ag_{38} are not as important as in the case of Ag_8. The oxygen atom gives rise to many transitions having a non-negligible intensity, but spectra of $Ag_{20}O$ and $Ag_{38}O$ are still dominated by an absorption band situated around 4.0 eV. However, the width of the main absorption band increases when oxygen atoms are added, and the spectrum of $Ag_{20}O_3$ ($Ag_{38}O_3$) strongly differs from the one of pure Ag_{20} (respectively Ag_{38}) cluster.

It is known that Ag_{20} and Ag_{38} have a plasmonic response in gas phase.[36] As suggested by Figure 2, oxidation leads to the decline of the plasmonic resonance on those clusters. This statement is also supported by experimental measurements. Lünskens et al[48] have used Second Harmonic Generation Spectroscopy (s-SHG) to study the effect of oxidation on supported silver clusters. They reported a significant decrease of s-SHG signal when clusters containing at least twenty silver atoms are exposed to oxygen. The spectra obtained by Lünskens et. al. on oxidized clusters are dominated by a wide absorption band and have similar shapes than the ones we calculated. A theoretical study using the Time-Dependent Density Functional Tight Binding method over aluminium nanoclusters also shows that oxidation lead to

an important decrease of plasmon resonance intensity,[49] which is in quantitative agreement with what we obtained with silver.

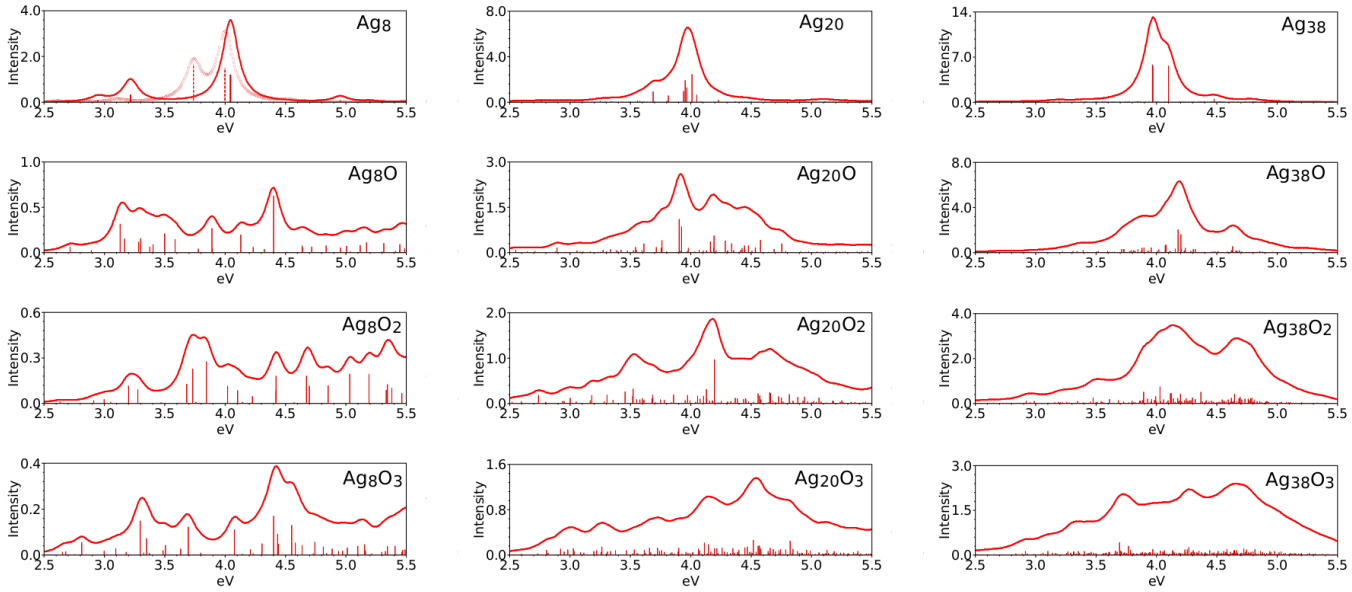


Figure 2: Absorption spectra of Ag_8, Ag_{20}, Ag_{38} (first row) and Ag_mO_n (m = 8, 20, 38, and n = 1, 2, 3). Spectra are plotted with a Lorentzian broadening (FWHM = 0.08 eV). For Ag_8 the solid lines (transitions and convolution) correspond to the spectrum of the T_d-symmetry isomer and the others (dashed transition and dotted convolution) to the spectrum of the D_{2d}-symmetry structure.

The density of states of pure Ag_{20} and Ag_{38} silver clusters, as well as the one of $Ag_{20}O$, $Ag_{20}O_2$, $Ag_{38}O$ and $Ag_{38}O_2$ are depicted in Figure 3. Some of the calculated Kohn-Sham orbitals are also represented in this figure. Our description of the density of states for oxidized silver cluster is in quantitative agreement with a previous DFT study concerning the oxidation of Ag_6.[28] It is well established that the electronic structure of silver clusters are in agreement with the shell model[19,50] in which the s valence electrons are distributed in delocalized orbitals with the following energy sequence : $1S^2$, $1P^6$, $1D^{10}$, $2S^2$, $1F^{14}$, $2P^6$, $1G^{18}$, etc. One can easily identify Kohn-Sham orbitals associated to different shells for pure Ag_{20} and Ag_{38}. The electronic structure of Ag_{20} ends with a full 2S shell, and the one of Ag_{38} ends with an open 2P shell. For the oxidized cluster, the $2p$ orbital of the oxygen, that we will note P_{Ox}, appears in the valence band of the silver cluster, leading to hybridization

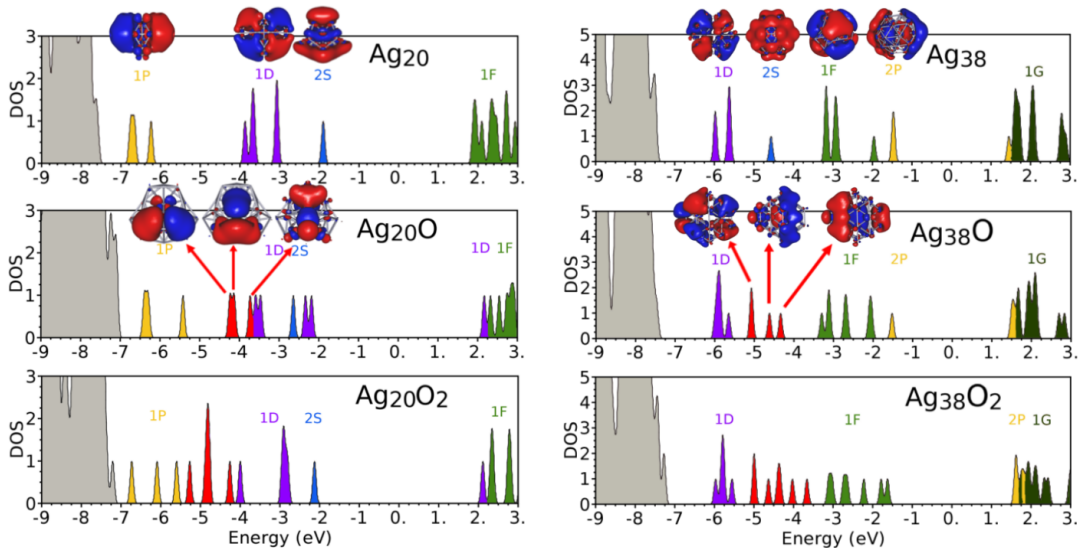


Figure 3: Density of states of Ag_{20}, $Ag_{20}O$, $Ag_{20}O_2$, Ag_{38}, $Ag_{38}O$, $Ag_{38}O_2$. The colours correspond to the different types of molecular orbitals, and the grey band represent the d electrons occupation. The molecular orbitals of type 1P, 1D and 2S for Ag_{20} as well as the 1D, 2S, 1F, 2P of Ag_{38} are drawn. The states having an important component over the oxygen atoms are in red, and the associated orbitals are represented for $Ag_{20}O$ and $Ag_{38}O$.

of those orbitals. In Figure 3, states that have a strong P_{Ox} character are represented in red and the corresponding orbitals are shown for $Ag_{20}O$ and $Ag_{38}O$. Since oxygen atoms attract electrons, some valence states of silver that are occupied in the case of pure silver cluster move to the conduction band when oxygen atoms are adsorbed. For Ag_{20}, some of the 1D orbitals become virtual when oxygen is added, and the adsorption of two oxygen atoms empty the whole 2P band of Ag_{38}. Hence, the presence of P_{Ox} orbitals in the valence band, with the subsequent hybridization between silver and oxygen orbitals, as well as the presence of new virtual states, leads to new optically allowed transitions which were not observed in pure metal clusters. Consequently, the absorption band is significantly broadened.

Oxidation induces a broadening and a damping of the plasmon band. The few intense transitions computed in the case of pure silver clusters are fragmented into many peaks which are scattered across a large range of frequencies when oxygen atoms are adsorbed. Figure 4 and Figure 5 show that this fragmentation is associated to the loss of the plas-

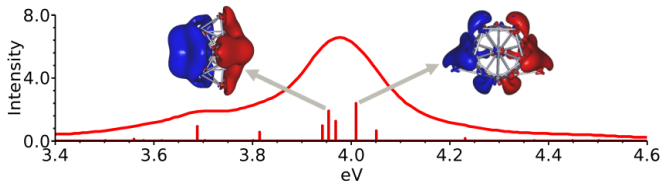


Figure 4: Absorption spectra of Ag_{20}. The isosurface plots of the transition density for two main peaks of Ag_{20}, situated at 3.95 and 4.01 eV, are represented. The red and blue surfaces respectively indicate positive and negative isovalues of $\pm$ 0.0003.

monic character of the excitations. A simple way to investigate the plasmonic character of an electronic transition is to plot its transition density.[36] The absorption spectra and the isosurface plot of the transition density of the two most intense excitations of Ag_{20} situated inside the main absorption band are given in Figure 4. The transition densities display a typical dipolar shape, which represents the oscillation of the electron density along the direction of the perturbative electric field. This type of signature is typical of excitation having an important plasmonic character.[36] Plots of the transition density of the five most intense peaks belonging to the main absorption band of $Ag_{20}O$ and $Ag_{20}O_2$ are represented in Figure 5. They reveal many alternations of positive and negative zones. The alternations of sign are more numerous for $Ag_{20}O_2$ than for $Ag_{20}O$. For oxidized clusters, the features of the density transition differ significantly from the ones found on the pure Ag_{20} cluster. This show that excitation computed on $Ag_{20}O$ and $Ag_{20}O_2$ do not have a strong plasmonic character. Thus the presence of oxygen atoms on the silver cluster induces a fragmentation of the plasmon resonance and replaces it by many excitations having a low plasmonic character.

Interestingly, the position of the oxygen atom with respect to the silver cluster has a non negligible effect over the optical properties. We built a structure of $Ag_{20}O$, hereafter noted $Ag_{20}O_{inside}$, where the oxygen is encapsulated inside the silver cluster. To do so, we replaced the only silver atom of Ag_{20} which is not at the surface with an oxygen atom and we added a silver atom at a random position on the cluster's surface. Then the geometrical structure has been relaxed with the ωB97x functional. The structure thereby obtained for $Ag_{20}O_{inside}$,

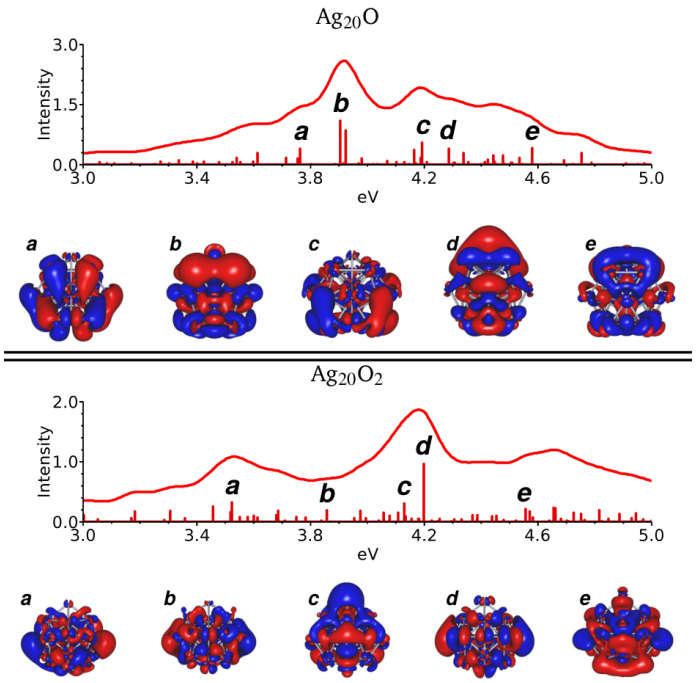


Figure 5: Absorption spectra of $Ag_{20}O$ (top) and $Ag_{20}O_2$ (bottom). Isosurface plots of the transition density (isovalue = $\pm$ 0.0003) of intense excitations (labeled *a,b,c,d,e*) are given below the spectra. Energy of represented transitions for $Ag_{20}O$ are 3.76 (a), 3.90 (b), 4.19 (c), 4.29 (d), and 4.58 (e) eV, those of $Ag_{20}O_2$ are 3.52 (a), 3.85 (b), 4.13 (c), 4.19 (d), and 4.57 (e) eV.

which is presented in Figure 6, lies 0.64 eV higher in energy compared to the lowest-energy isomer of $Ag_{20}O$. This suggests that oxygen atoms preferably stay at the cluster's surface, which is in agreement with previous DFT study.[27,28] The electric charge on the oxygen atom placed inside Ag_{20} is -1.24 $|e|$. The density of state and the absorption spectrum of $Ag_{20}O_{inside}$ is given in Figure 6. The ordering of the orbitals is the same than for $Ag_{20}O$, shown in Figure 3. The spectra of $Ag_{20}O_{inside}$ and $Ag_{20}O$ present some similarities. In both cases many transitions appear in the main absorption band compared to the spectrum of pure Ag_{20}. However, the induced broadening is not as important in the case of $Ag_{20}O_{inside}$ than it is in the case of $Ag_{20}O$. When the oxygen atom is inside the silver cluster the intense transitions are all positioned between about 3.8 and 4.2 eV. By comparison, when the oxygen atom is adsorbed at the surface, the important transitions lie in an energy range that is at least twice larger. Isosurface plots of the transition density of five peaks of the

$Ag_{20}O_{inside}$ spectrum are given in the Figure 6. These transition densities do not show as many alternations of sign as in the case of $Ag_{20}O$. They are globally distributed in two zones, having opposite sign, on both side of the system, i.e. a somewhat dipolar shape. This type of distribution proofs that, despite of the presence of the oxygen atom, the intense transitions for $Ag_{20}O_{inside}$ have a plasmonic character. In contrast, the presence of O atoms at the surface prevents the formation of a dipolar mode.

The role the relative position of O atoms has already been discussed by Burgel et al[31] when investigating the oxidation of very small silver clusters as Ag_4. They concluded that structures with centrally located oxygen atom, and structures where the oxygen is strongly coordinated with multiple neighbours, present a absorption spectrum relatively similar to that of the pure silver cluster. Contrastingly, when the oxygen atom is located in a peripheral position, several new intense peaks spread over a large energy range become visible due to a stronger activation of d-electrons of Ag atoms by p-electrons of the O atom. Our results confirm their statement.

We also studied the interaction between molecular O_2 and Ag_8 as well as the impact of this molecule on the optical response of this cluster. We focused on Ag_8 as it is the smallest cluster we considered in this paper, and so it is likely the most sensitive to the chemical interactions. Experiments on the interaction of gas phases of silver clusters with O_2 have shown that molecular O_2 can be either physisorbed or chemisorbed on small cationic silver clusters.[25,26] DFT studies of silver cluster Ag_n in interaction with molecular O_2 reveal that dioxygen can be adsorbed at either atop (only one O-Ag bond) or bridge (each O are bound to the cluster) sites, depending on cluster's size and charge.[27–29] Those theoretical studies also reveal that the dissociative adsorption (DA) is favored for $n \geq 6$, i.e. the binding energies for molecular adsorption is lower than DA's energies when the silver cluster is large enough to transfer electrons to oxygen atoms. We have considered the attachment of molecular dioxygen on the T_d-symmetry structure of Ag_8. Two types of adsorption were considered: one with the dioxygen in an atop site, and the other one with O_2 in a bridge

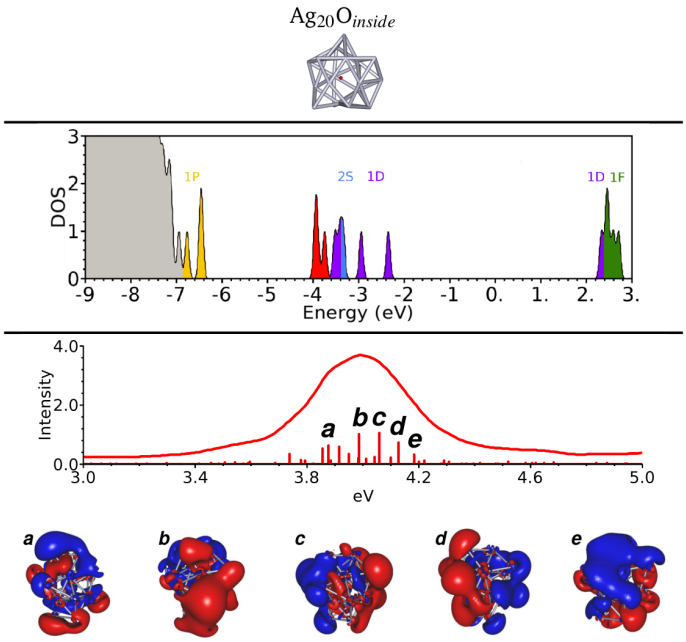


Figure 6: Geometry (top), density of states (middle) of $Ag_{20}O_{inside}$, together with the absorption spectrum and the density transition (isovalue = $\pm$ 0.0003) of five intense peaks (bottom). For the density of states, the grey band corresponds to the *d* electrons, the red states to orbitals that have an important component over the oxygen atom, and others colours to the different shells. The transition densities labeled in the absorption spectra correspond to excitation situated at 3.88 (a), 3.99 (b), 4.06 (c), 4.13 (d) and 4.18 (e) eV.

position. The geometrical structures and the absorption spectra of pure Ag_8, and Ag_8 in interaction with molecular O_2 are given in Figure 7. In all cases, the geometrical configuration obtained with molecular O_2 is not as steady as the one obtained with two dissociated oxygen atoms. For Ag_8 in interaction with dioxygen on an atop site, the steadiest electronic configuration corresponds to a spin multiplicity of three. For this isomer (Figure 7b), the dioxygen does not induce a strong deformation of the cluster, the binging energy is +0.17 eV, and the Ag-O distance is 2.82 Å. In the atop position, the oxygen atoms are separated of 1.22 Å, i.e. an elongation of only 0.02 Åcompared to O_2 in gas phase. A singlet state is also found (Figure 7c), it lies 0.15 eV below the dissociation limit of Ag_8 + O_2(singlet) and the Ag-O distance is 2.47 Å. For Ag_8 interacting with dioxygen on a bridge site, the steadiest electronic configuration corresponds to a multiplicity of three (Figure 7d). The configuration lies 0.24 eV below the dissociation limit. The O-O bond is elongated to 1.31 Å, while

the shortest O-Ag distances are 2.31 and 2.24 Å. In the bridge position, the net charge on oxygen atom is -0.32 $|e|$ per atom, and that transfer of electron suggests a chemisorption state. The hybridization between the orbitals of the silver cluster and the ones of the dioxygen are important when O_2 is in the bridge position, while it is very low for O_2 in an atop site.

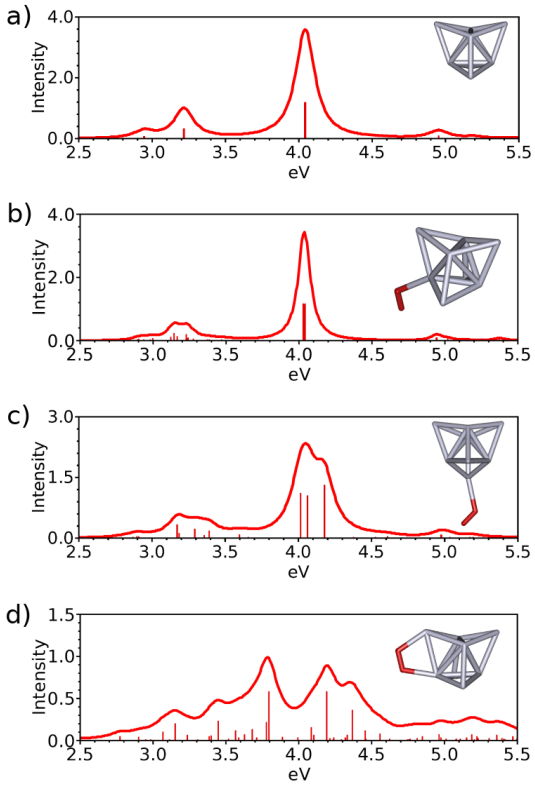


Figure 7: Geometry and absorption spectra of pure Ag_8 in the T_d symmetry (a). Geometry and absorption spectra of Ag_8 in interaction with molecular O_2 at the atop position in a triplet state (b), or a singlet state (c), and with O_2 in the bridge position (d).

Figure 7 shows that the adsorption of O_2 in an atop position does not induce significant changes in the absorption spectra of Ag_8. The main transitions of Ag_8 in the T_d symmetry are three times degenerated and are situated at 3.22, 4.04, and 4.96 eV respectively. With the molecular O_2 in an atop position, the system is not in a T_d symmetry anymore, and the degeneracy is raised. For the triplet state, O_2 is far from silver atoms and the spectrum stay very similar to the one of pure metal cluster (Figure 7b). In the singlet state, the peaks of Ag_8 are clearly fragmented, leading to an widening of the bands. The main bands

are centered at 3.2, 4.1, 5.0 eV respectively (Figure 7c). In both case, the spectrum of Ag_8 is quite recognizable. This can be understood by the fact that the molecular O_2 is physisorbed in the atop position and thus the orbitals of the silver and oxygen atoms are weakly hybridized. In contrast the absorption spectrum changes significantly (Figure 7d) when the two oxygen atoms bind to the metal cluster. The absorption spectra is dominated by a large band between 3 and 4.5 eV, with two main peaks at 3.80 and 4.2 eV, followed by a non-negligible tail until 5.5 eV. The strong hybridization between silver and oxygen leads to a significant electronic reorganization. Figure 7 reveals that the changes induced by the O_2 molecule on the optical response strongly depends on how it is bound to the cluster.

Conclusions

The optical response of oxidized clusters, containing 8, 20 or 38 silver atoms have been calculated at TDDFT/RSH level. Oxidation is found to induce hybridization and rearrangements in the orbital filling, leading to significant changes on the optical response. Oxygen atoms induce a strong damping and broadening of the absorption band, and can even lead to its disappearance. The broadening of the absorption band is characterized by the fact that the few strong transitions with an important plasmonic character in pure silver clusters are replaced by many transitions spread over a wide range of energy and having low plasmonic character. These new transitions originate from the presence of oxygen orbitals in the valence states, the presence of new virtual states subsequent to charge transfers, and also from hybridization between silver and oxygen orbitals. The damping is all the more important when the number of oxygen atoms is large. However, the effects are reduced when oxygen atom is located inside the metal cluster.

We have also studied the interactions between Ag_8 and molecular O_2 and demonstrated that changes induced by the molecular adsorption on the absorption spectrum strongly depend on the adsorption mode. Thus spectroscopic measurements seem to be relevant to

study oxidation process and to discriminate the adsorption modes on metallic clusters.

The present work can be view as a first step to model precisely the effects of an oxide matrice on the optical response of silver clusters. It is worth to emphasize that one should expect a significant damping to the plasmonic response for cluster embedded in those matrices compared to gas phase measurement if chemical bonds are formed between silver and oxygen atoms. From the present study, it can be expected that the adsorption of oxygen atoms on small metal clusters prevents the detection of the plasmon band.

Acknowledgement

This work was performed using HPC resources from GENCI-IDRIS (Grant A0050807662) and the Pôle Scientifique de Modélisation Numérique (PSMN). It has received a financial support from the French National Research Agency (Agence Nationale de la Recherche, ANR) in the frame of the project FIT SPRINGS, ANR-14-CE08-0009. The authors gratefully acknowledge A.R. Allouche for support for the use of Gabedit.

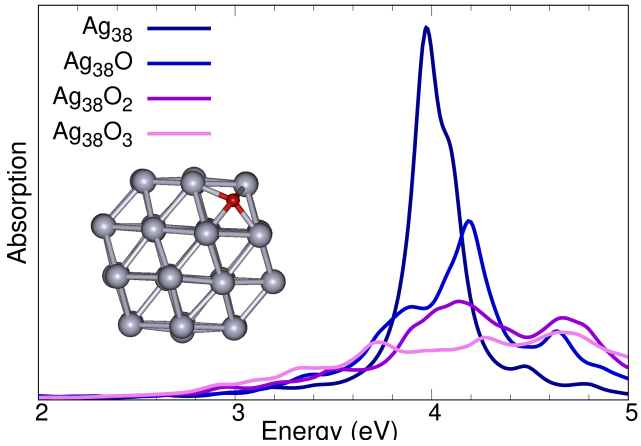


Table of Contents Graphic (TOC)

References

(1) Schwartzberg, A. M.; Zhang, J. Z. Novel optical properties and emerging applications of metal nanostructures. *The Journal of Physical Chemistry C* **2008**, *112*, 10323–10337.

(2) Mathew, A.; Pradeep, T. Noble metal clusters: applications in energy, environment, and biology. *Particle & Particle Systems Characterization* **2014**, *31*, 1017–1053.

(3) Zhang, J.-Z. Biomedical applications of shape-controlled plasmonic nanostructures: a case study of hollow gold nanospheres for photothermal ablation therapy of cancer. *The Journal of Physical Chemistry Letters* **2010**, *1*, 686–695.

(4) Lim, W. Q.; Gao, Z. Plasmonic nanoparticles in biomedicine. *Nano Today* **2016**, *11*, 168 – 188.

(5) Zeng, S.; Yong, K.-T.; Roy, I.; Dinh, X.-Q.; Yu, X.; Luan, F. A review on functionalized gold nanoparticles for biosensing applications. *Plasmonics* **2011**, *6*, 491–506.

(6) Sarina, S.; Waclawik, E. R.; Zhu, H. Photocatalysis on supported gold and silver nanoparticles under ultraviolet and visible light irradiation. *Green Chemistry* **2013**, *15*, 1814–1833.

(7) Stamplecoskie, K. G.; Scaiano, J. C.; Tiwari, V. S.; Anis, H. Optimal size of silver nanoparticles for surface-enhanced Raman spectroscopy. *The Journal of Physical Chemistry C* **2011**, *115*, 1403–1409.

(8) Leng, W.; Vikesland, P. J. Nanoclustered gold honeycombs for surface-enhanced Raman scattering. *Analytical Chemistry* **2013**, *85*, 1342–1349.

(9) Atwater, H. A.; Polman, A. Plasmonics for improved photovoltaic devices. *Nature Materials* **2010**, *9*, 205–213.

(10) Jeseentharani, V.; Pugazhenthiran, N.; Mathew, A.; Chakraborty, I.; Baksi, A.; Ghosh, J.; Jash, M.; Anjusree, G. S.; Deepak, T. G.; Nair, A. S. et al. Atomically precise noble metal clusters harvest visible light to produce energy. *ChemistrySelect* **2017**, *2*, 1454–1463.

(11) Haberland, H. Looking from both sides. *Nature* **2013**, *494*, E1.

(12) Sinha-Roy, R.; García-González, P.; Weissker, H.-C.; Rabilloud, F.; Fernández-Domínguez, A. I. Classical and ab initio plasmonics meet at sub-nanometric noble metal rods. *ACS Photonics* **2017**, *4*, 1484–1493.

(13) Hövel, H.; Fritz, S.; Hilgerand, A.; Kreibig, U.; Vollmer, M. Width of cluster plasmon resonances: bulk dielectric functions and chemical interface damping. *Physical Review B* **1993**, *48*, 18178–18188.

(14) Campos, A.; Troc, N.; Cottancin, E.; Pellarin, M.; Weissker, H.-C.; Lermé, J.; Kociak, M.; Hillenkamp, M. Plasmonic quantum size effects in silver nanoparticles are dominated by interfaces and local environments. *Nature Physics* **2018**, *15*, 275–280.

(15) Tiggesbäumker, J.; Köller, L.; Meiwes-Broer, K.-H.; Liebsch, A. Blue shift of the Mie plasma frequency in Ag clusters and particles. *Physical Review A* **1993**, *48*, 1749–1752.

(16) Hilger, A.; Cüppers, N.; Tenfelde, M.; Kreibig, U. Surface and interface effects in the optical properties of silver nanoparticles. *European Physical Journal D* **2000**, *10*, 115–118.

(17) Lünskens, T.; Heister, P.; Walenta, M. T. C. A.; Kartouzian, A.; Heiz, U. Plasmons in supported size-selected silver nanoclusters. *Physical Chemistry Chemical Physics* **2015**, *17*, 17541–17544.

(18) Chakraborty, I.; Erusappan, J.; Govindarajan, A.; Sugi, K. S.; Udayabhaskararao, T.;

Ghosh, A.; Pradeep, T. Emergence of metallicity in silver clusters in the 150 atom regime: a study of differently sized silver clusters. *Nanoscale* **2014**, *6*, 8024–8031.

(19) Yu, C.; Schira, R.; Brume, H.; von Issendorff, B.; Rabilloud, F.; Harbich, W. Optical properties of size selected neutral Ag clusters: electronic shell sructures and the surface plasmon resonance. *Nanoscale* **2018**, *10*, 20821–20827.

(20) Genzel, L.; Martin, T. P.; Kreibig, U. Dielectric function and plasma resonances of small metal particles. *Zeitschrift für Physik B Condensed Matter* **1975**, *21*, 339–346.

(21) Gaudry, M.; Lermé, J.; Cottancin, E.; Pellarin, M.; Vialle, J. L.; Broyer, M.; Prével, B.; Treilleux, M.; Mélinon, P. Optical properties of $(Au_xAg_{1-x})_n$ clusters embedded in alumina: Evolution with size and stoichiometry. *Physical Review B* **2001**, *64*, 085407.

(22) Cottancin, E.; Celep, G.; Lermé, J.; Pellarin, M.; Huntzinger, J. R.; Vialle, J. L.; Broyer, M. Optical properties of noble metal clusters as a function of the size: comparison between experiments and a semi-quantal theory. *Theoretical Chemistry Accounts* **2006**, *116*, 514–523.

(23) Hillenkamp, M.; Domenicantonio, G. D.; O.Eugster,; Félix, C. Instability of Ag nanoparticles in SiO_2 at ambient conditions. *Nanotechnology* **2006**, *18*, 015702.

(24) Lermé, J. Size evolution of the surface plasmon resonance damping in silver nanoparticles: confinement and dielectric effects. *The Journal of Physical Chemistry C* **2011**, *115*, 14098–14110.

(25) Schmidt, M.; Masson, A.; Bréchignac, C. Oxygen and silver clusters: tansition from chemisorption to oxidation. *Physical Review Letter* **2003**, *91*, 243401.

(26) Schmidt, M.; Bréchignac, C. Silver and oxygen: Transition from clusters to nanoparticles. *Comptes Rendus Physique* **2016**, *17*, 481–484.

(27) Wang, Y.; Gong, X.-G. First-principles study of small oxidized silver clusters. *Journal of Nanoscience and Nanotechnology* **2010**, *10*, 5500–5506.

(28) Klacar, S.; Hellman, A.; Panas, I.; Grönbeck, H. Oxidation of small silver clusters: a density functional theory study. *The Journal of Physical Chemistry C* **2010**, *114*, 12610–12617.

(29) Liao, M.-S.; Watts, J. D.; Huang, M.-J. Theoretical comparative study of oxygen adsorption on neutral and anionic Ag_n and Au_n clusters (n = 2–25). *The Journal of Physical Chemistry C* **2014**, *118*, 21911–21927.

(30) Bonačić-Koutecký, V.; Boiron, M.; Pittner, J.; Fantucci, P.; Koutecký, J. Structural and optical properties of small oxygen-doped- and pure-silver clusters. *The European Physical Journal D* **1999**, *9*, 183–187.

(31) Bürgel, C.; Mitrić, R.; Bonačić-Koutecký, V. Emissive properties of silver particles at silver oxide surface defects. *Applied Physics A* **2006**, *82*, 117–123.

(32) Casida, M. E. *Recent advances in density functional methods*; World Scientific, 1995; pp 155–192.

(33) Rabilloud, F. Assessment of the performance of long-range-corrected density functionals for calculating the absorption spectra of silver clusters. *The Journal of Physical Chemistry A* **2013**, *117*, 4267–4278.

(34) Kuisma, M.; Sakko, A.; Rossi, T.; Larsen, A. H.; Enkovaara, J.; Lehtovaara, L.; Rantala, T. T. Localized surface plasmon resonance in silver nanoparticles: Atomistic first-principles time-dependent density-functional theory calculations. *Physical Review B* **2015**, *91*, 115431.

(35) Baseggio, O.; Vetta, M. D.; Fronzoni, G.; Stener, M.; Sementa, L.; Fortunelli, A.; Calzolar, A. Photoabsorption of icosahedral noble metal clusters: an efficient TDDFT

approach to large-scale systems. *Journal of Physical Chemistry C* **2016**, *120*, 12773–12782.

(36) Schira, R.; Rabilloud, F. Localized surface plasmon resonance in free silver nanoclusters Ag_n, $n = 20$–147. *The Journal of Physical Chemistry C* **2019**, *123*, 6205–6212.

(37) Dreuw, A.; Head-Gordon, M. Failure of time-dependent density functional theory for long-range charge-transfer excited states: the zincbacteriochlorin-bacteriochlorin and bacteriochlorophyll-spheroidene complexes. *Journal of the American Chemical Society* **2004**, *126*, 4007–4016.

(38) Rabilloud, F. Description of plasmon-like band in silver clusters: The importance of the long-range Hartree-Fock exchange in time-dependent density-functional theory simulations. *The Journal of Chemical Physics* **2014**, *141*, 144302.

(39) Chai, J.-D.; Head-Gordon, M. Systematic optimization of long-range corrected hybrid density functionals. *The Journal of Chemical Physics* **2008**, *128*, 084106.

(40) Hay, P. J.; Wadt, W. R. Ab initio effective core potentials for molecular calculations. Potentials for K to Au including the outermost core orbitals. *The Journal of Chemical Physics* **1985**, *82*, 299–310.

(41) Schira, R.; Rabilloud, F. Effects of rare-gas matrices on the optical response of silver nanoclusters. *The Journal of Physical Chemistry C* **2018**, *122*, 27656–27661.

(42) Hariharan, P. C.; Pople, J. A. The influence of polarization functions on molecular orbital hydrogenation energies. *Theoretica Chimica Acta* **1973**, *28*, 213–222.

(43) Chen, M.; Dyer, J. E.; Li, K.; Dixon, D. A. Prediction of structures and atomization energies of small silver clusters, Ag_n, $n < 100$. *The Journal of Physical Chemistry A* **2013**, *117*, 8298–8313.

(44) Harb, M.; Rabilloud, F.; Simon, D.; Rydlo, A.; Lecoultre, S.; Conus, F.; Rodrigues, V.; Félix, C. Optical absorption of small silver clusters: Ag_n, (n=4–22). *The Journal of Chemical Physics* **2008**, *129*, 194108.

(45) Frisch, M. J.; Trucks, G. W.; Schlegel, H. B.; Scuseria, G. E.; Robb, M. A.; Cheeseman, J. R.; Scalmani, G.; Barone, V.; Petersson, G. A.; Nakatsuji, H. et al. Gaussian 09 Revision D.01. 2009; Gaussian Inc. Wallingford CT.

(46) Allouche, A.-R. Gabedit—A graphical user interface for computational chemistry softwares. *Journal of Computational Chemistry* **2011**, *32*, 174–182.

(47) Reed, A. E.; Weinstock, R. B.; Weinhold, F. Natural population analysis. *The Journal of Chemical Physics* **1985**, *83*, 735–746.

(48) Lünskens, T.; Walenta, C. A.; Heister, P.; Kartouzian, A.; Heiz, U. Surface oxidation of supported, size-selected silver clusters. *Journal of Cluster Science* **2017**, *28*, 3185–3192.

(49) Douglas-Gallardo, O. A.; Soldano, G. J.; Mariscal, M. M.; Sanchez, C. G. Effects of oxidation on the plasmonic properties of aluminum nanoclusters. *Nanoscale* **2017**, *9*, 17471–17480.

(50) de Heer, W. A. The physics of simple metal clusters: experimental aspects and simple models. *Reviews of Modern Physic* **1993**, *65*, 611–676.